

## Perspective/Review

Physicochemical properties of bacterial glycopolymers in relation to  
bioactivityKlaus Brandenburg,<sup>a,\*</sup> Jörg Andrä,<sup>a</sup> Mareike Müller,<sup>a</sup> Michel H.J. Koch,<sup>b</sup>  
Patrick Garidel<sup>c</sup><sup>a</sup> Forschungszentrum Borstel, LG Biophysik, Parkallee 10, D-23845 Borstel, Germany<sup>b</sup> European Molecular Biology Laboratory, Notkestr. 52, D-22603 Hamburg, Germany<sup>c</sup> Universität Halle-Wittenberg, Inst. für Physikalische Chemie, Mühlpforte 1, D-06108 Halle, Germany

Received 10 April 2003; accepted 11 August 2003

## Abstract

An overview is given on the physicochemical properties of bacterial glycopolymers, i.e., pure oligo- and polysaccharides as well as glycolipids. Data from analysis of the chemical and physicochemical properties of various sugar polymers are summarized. Furthermore, data are presented on the thorough characterization of the most important class of bacterial glycopolymers, the lipopolysaccharides (LPS). These data comprise the chemical characterization, the gel to liquid crystalline phase transition behaviour of their acyl chains, the ultrastructural studies of their morphology, and the investigation of the types of aggregate structures present above the critical micellar concentration (CMC). Furthermore, the relevance of these data with respect to an understanding of the various biological effects elicited by LPS is discussed.

© 2003 Elsevier Ltd. All rights reserved.

**Keywords:** Glycoconjugates; Bacterial polysaccharides; Lipopolysaccharides; Endotoxins; Cytokines

## Contents

1. Introduction	2477
2. Microbial glycopolymers	2478
2.1. Microbial polysaccharides	2478
2.1.1. Chemical analyses	2478
2.1.2. Physico-chemical analyses	2479
2.2. Glycolipids/lipopolysaccharides	2479
2.2.1. Chemical characterization of glycolipids	2481
2.2.2. $\beta \leftrightarrow \alpha$ acyl chain melting transition of endotoxins	2481
2.2.3. General ultrastructural studies	2482
2.2.4. CMC and aggregate structure of endotoxins	2484
2.2.5. Correlations to bioactivity	2487
References	2488

## 1. Introduction

Glycopolymers are sugar-containing compounds, which may consist of repeating units of mono- or oligosaccharides (chemical glycopolymers) or which are sugar-containing macromolecules which in aqueous suspensions form polymeric aggregates (physical glycopoly-

\* Corresponding author. Tel.: +49-4537-188235; fax: +49-4537-188632.

E-mail address: [kbranden@fz-borstel.de](mailto:kbranden@fz-borstel.de) (K. Brandenburg).

mers). Of course, the chemical glycopolymers may also be able to form physical glycopolymers. The glycoconjugates, glycolipids and glycoproteins, belong to the second class, as the most important group. The biological importance of this class has become evident only in the last 20 years. Glycolipids are essential constituents of cellular membranes with a large number of functions.<sup>1–3</sup> They may act as receptors, may provide specific contact, be important for cell aggregation and dissociation, and may transmit and receive signals, for example to initiate cell division. Cerebrosides and monoacylglucosides belong to the simple glycolipids, and gangliosides belong to the more complex glycolipids, which usually have specialized functions as, e.g., as cell surface receptors. Many glycolipids are known to modulate the immune response. In common nomenclature also bacterial lipopolysaccharides (LPS, endotoxins) belong to this class. LPS induce a variety of biological effects in mammals like activation of mononuclear cells to produce cytokines such as tumor necrosis factor and interleukins.<sup>4</sup>

Glycoproteins, i.e., proteins with a covalently linked carbohydrate moiety, are also ubiquitous in nature. They are found in cell membranes and inside cells, in the cytoplasm as well as in subcellular organelles and in extracellular fluids. Blood is one of the main sources of glycoproteins, and nearly all of the almost 100 proteins identified there are glycosylated. The carbohydrate content of glycoproteins may vary strongly, from less than 1 to over 99% and may consist of a mono- up to a polysaccharide (glycan), linear or branched. In most cases, individual glycoproteins usually carry different saccharides at the same attachment site in the polypeptide chain. Therefore, heterogeneity of the carbohydrates is the rule. Peptidoglycans and/or glycopeptides, a sub-class of the glycoproteins, are important constituents of the bacterial cell wall (murein layer). They are mainly responsible for the mechanical stability of the bacterial cells, and their amount, for Gram-positive bacteria, may be as high as 50% of the mass of the cell envelope.

## 2. Microbial glycopolymers

### 2.1. Microbial polysaccharides

A large number of microorganisms, from archaebacteria over unicellular algae to soil bacteria produce extracellular or capsular polysaccharides with high molecular weight, which may be either neutral or charged. Many of the microbial polysaccharides can be distinguished from other carbohydrate polymers by the existence of regular repeating units of oligosaccharides, branched or unbranched, with specific glycosidic linkages between the single monosaccharides. These macromolecules may,

even in dilute solutions, assume ordered conformations, such as stable gels or lyotropic liquid crystals.

Usually, the polysaccharides are produced either as extracellular chains, or belong to the cell envelope of the bacteria as capsular ones. Important groups of polysaccharides found in microbes are the glucuronans, the xanthans, hyaluronic acid and heparin-like compounds, alginates and the gellans. An overview on microbial polysaccharides of applied interest is given by Crescenzi.<sup>5</sup> Furthermore, the characterization of polysaccharides by the application of vibrational spectroscopy has been reviewed by Brandenburg and Seydel.<sup>6</sup>

**2.1.1. Chemical analyses.** The basic techniques for chemical analyses are shortly summarized here. The glucose content of glycopolymers can be measured by the orcinol reaction.<sup>7</sup> Phosphorus can be determined according to the method of Chen and coworkers,<sup>8</sup> and phosphate monoesters specifically, can be determined by measuring the inorganic phosphate released by potato acid phosphatase.<sup>9</sup> The analysis of reducing sugars can be made according to Park and Johnson,<sup>10</sup> and the sialic acid content of oligosaccharides can be monitored by a modified Svennerholm method.<sup>11</sup> The O-acetyl content can be estimated according to the method of Hestrin.<sup>12</sup> Formaldehyde, released from oligosaccharides, can be determined after O-deacetylation and periodate treatment as described.<sup>13,14</sup> A quantitative analysis of sugar constituents of oligosaccharide by means of capillary electrophoresis was presented recently by Chen and coworkers,<sup>15</sup> and an ultrasensitive chemical method for polysialic acid analysis was presented by Inoue and coworkers.<sup>16</sup> High resolution and high sensitivity methods for oligosaccharide mapping and sugar characterization by normal phase high performance chromatography was presented by Anumula and Dhume.<sup>17</sup>

The combination of a variety of techniques allows the determination of the complete structure of a polysaccharide. Thus, for example, Sato and coworkers<sup>18</sup> established a novel structure of a bacterial cell-wall polysaccharide from a Gram-positive bacterium. The structure of the antigenic polysaccharide produced by *Eubacterium saburreum* T15 was determined using acid

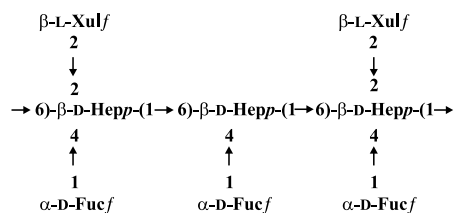


Fig. 1. Repeating unit of a cell-wall antigenic polysaccharide from the Gram-positive species *E. saburreum* (adapted from Sato and coworkers<sup>18</sup>). Xul = L-threo-pent-2-ulose; Fuc = D-fucose; Hep = D-glycero-D-galacto-heptose.

hydrolysis, methylation analysis, and 1D and 2D NMR spectroscopy. It contained *L*-threo-pent-2-ulose (Xul), *D*-fucose (Fuc), and *D*-glycero-*D*-galacto-heptose (Hep) in 2:3:3 ratios. Methylation analysis indicated an octasaccharide repeating unit containing five branches. The polysaccharide also contains two *O*-acetyl groups in the repeating unit, located on the Hep residue (Fig. 1). Another example is that by Varbanets and coworkers<sup>19</sup> who were able, using various analyzing techniques, to perform a biochemical characterization of phosphorus-containing glycopolymers from *Clavibacter michiganese* cell walls. Such information on the monosaccharide composition of cell-wall polysaccharides of coryneform bacteria can be used to classify these organisms with respect to genus and species.

**2.1.2. Physico-chemical analyses.** Ion exchange chromatography can be used for the determination of the aggregate size of oligosaccharides.<sup>20</sup> Efforts are put in size fractionation of bacterial capsular polysaccharides, because of their use for the development of vaccines.<sup>21</sup> Bussat and coworkers<sup>22</sup> have used high-performance liquid chromatography (HPLC) for the characterisation of the molecular size of bacterial capsular polysaccharide vaccines, since the molecular size is an important physico-chemical criterion which correlates with immunogenicity. The distribution coefficient of different polysaccharides (*Haemophilus*-type b and various pneumococcal types) were determined and compared to data obtained from GPC (see Table 1 in Bussat and coworkers<sup>22</sup>). The authors were able to show that their HPLC method is rapid, accurate, and reproducible, requires only low amounts of sample and presents good correlation with data from conventional GPC. The latter method is time consuming and requires large amounts of sample. Information concerning the physico-chemical organisation of polysaccharide-supported planar bilayer lipid model membranes can be made visible by means of fluorescence microscopy and reflection interference contrast microscopy.<sup>23</sup>

## 2.2. Glycolipids/lipopolysaccharides

The main class of bacterial glycolipids is the LPS, which is located on the surface of the outer membrane of Gram-negative bacteria (it should be noted here, however, that LPS is sometimes considered to represent a class different from glycolipids).<sup>6</sup> The LPS is essential for the physiological membrane functions of the bacterium and also for its growth and survival.<sup>4</sup> It contributes to the low membrane permeability and enhances the resistance towards hydrophobic agents. The LPS contributes to the biosynthesis of outer membrane proteins (OMPs, porins) and are important for their correct functioning. At the same time, it is the primary target for the interaction with antibacterial drugs and compo-

nents of the immune system of the host (Fig. 2). When released by the attack of the immune cells or simply by the division of cells, the LPS is able to induce a variety of biological effects when administered to animals or humans or in vitro. The result of the specific interaction of LPS with cells was the activation of cells such as cellular proliferation of B-lymphocytes, the formation and secretion of bioactive mediators (cytokines) as produced by monocytes, macrophages, and vascular cells (Fig. 2).<sup>4</sup> At low concentrations these mediators are beneficial for the proper functioning of the immune system and its fight against invading microorganisms, at high concentrations, however, these mediators cause toxic effects such as pyrogenicity, leukopenia, and irreversible shock. Thus, the LPS plays an important role in the pathogenesis and manifestation of Gram-negative infection and in particular of septic shock and are therefore also termed endotoxins. Chemically, the LPS consists of a hydrophilic polysaccharide covalently linked to a hydrophobic lipid portion, termed lipid A, which anchors the molecule in the outer membrane. In wild type strains, the polysaccharide portion consists of an *O*-specific chain and the core oligosaccharide (S-form LPS). Rough mutant strains do not express the *O*-specific chain, but have core oligosaccharides of varying length, which are characterized by chemotypes in the sequence of decreasing length of the core sugar as Ra (complete core), Rb, Rc, Rd, and Re (Fig. 3).<sup>24</sup> The latter, deep rough mutant LPS, represents the minimal structure of LPS consisting only of lipid A and two 3-deoxy-*D*-manno-oct-2-ulopyranosonic acid (= 2-keto-3-deoxyoctonate, Kdo) monosaccharides. The usually high negative charge of the LPS molecules makes them an important target especially for polycationic antibacterial peptides, which are discussed as new possible antiseptic drugs.

As stressed above, the LPS is, after removal from the outer membrane, one of the most potent agents to trigger the immune system and to induce cytokines in immunocompetent cells. In the light of this observation, attempts have been made to correlate the specific chemical structure of these macromolecules with their biological activity. From these investigations it was deduced that the lipid A part was the 'endotoxic principle', and that the polysaccharide portion of LPS of the cell wall of enterobacteria was considered to be a solubilizing carrier for the biologically active part. In contrast to the role of varying sugar content, alterations of the lipid A moiety were found to influence the bioactivity dramatically leading for example for a lipid A with less than six acyl chains to complete inactivity.<sup>25</sup> However, these lipid A variants such as the tetraacyl lipid A IVa or synthetic compound '406' can act antagonistically, i.e., can block the action of agonistically active LPS.

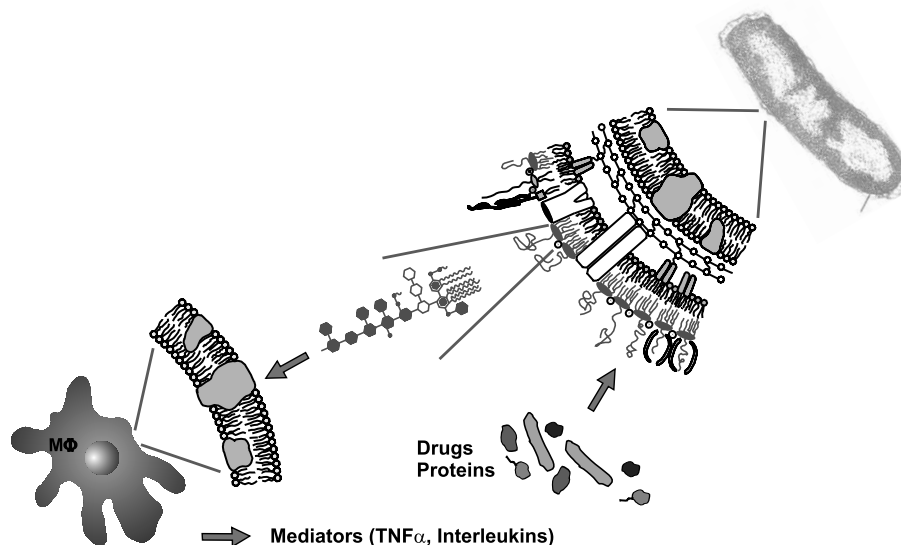


Fig. 2. Schematic representation of the activation mechanisms induced by LPS. LPS is released from the bacterial outer membrane by the attack of immune components (drugs, proteins) or simply by cell division. It may interact with serum and membrane proteins, which subsequently leads to an activation of macrophages, which secrete mediators such as tumor-necrosis-factor- $\alpha$  and interleukins.

Here, the basic physico-chemical prerequisites of endotoxically active and inactive LPS are described. This comprises the experimental determination of the chemical structure, the supramolecular three-dimensional aggregate structure, the latter allowing the determination of the molecular shape (conformation), and the intramolecular conformation.

Endotoxins (LPS and lipid A) as amphiphilic molecules form aggregates in aqueous environments above a critical concentration (critical micellar concentration, CMC), depending among other things on their hydrophobicity.<sup>26</sup> The actual structure of these aggregates depends on the conformation (shape) of the contributing molecules, which is again determined by their

primary chemical structure and is influenced by ambient conditions like temperature, pH, water content, and concentration of mono- and divalent cations. The molecular shape of a given amphiphilic molecule like LPS or lipid A within a supramolecular aggregate is not a constant but will depend, at least in part, on the fluidity (inversely correlated to the state of order) of its acyl chains which can assume two main phase states, the well known gel ( $\beta$ ) phase and liquid-crystalline ( $\alpha$ ) phase. At a characteristic phase transition temperature  $T_c$ , a reversible transition between these two phases takes place.  $T_c$  depends on the length and the degree of saturation of the acyl chains as well as on the conformation and the charge density of and their

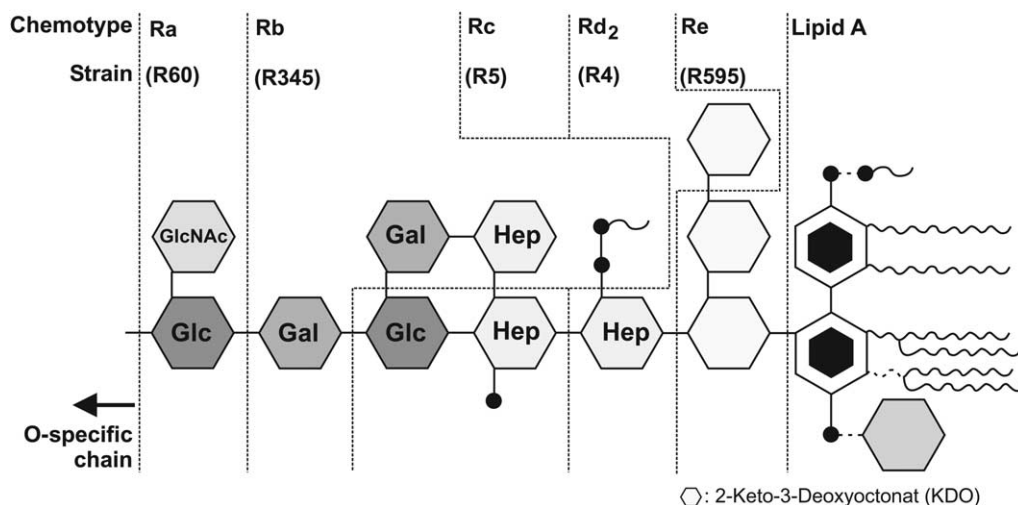


Fig. 3. Schematic structure of various mutant LPS from *S. minnesota*. The length of the oligosaccharide part decreases in the chemotype sequence Ra, Rb, Rc, Rd, and Re, the corresponding strains from *S. minnesota* are R60, R345, R5, R4, and R595.



distribution within the head group region. From the variability in the acylation patterns and composition of the sugar moiety, a complex phase behaviour and structural polymorphism are to be expected for free lipid A and for LPS.

**2.2.1. Chemical characterization of glycolipids.** It can be generally stated that the structural variability is lowest for the lipid A part ('conservative' structure), higher in the core oligosaccharide, and highest in the O-polysaccharide chain.<sup>27</sup> The variability of the core oligosaccharide and even more of the O-polysaccharide between different bacterial strains and genera, is indicative of the main role of the sugar part as epitopes for antibody binding and as steric hindrance for hydrophobic drugs thus contributing to the permeability barrier of the bacterial cell.<sup>4</sup>

The only structural element that is present in all core regions is the Kdo residue which links the lipid A part with the residual sugar oligo- or polysaccharide. The core structures of single genus are relatively homogeneous, for example for *Salmonella enterica*, all further monosaccharides consist of L-glycero-D-manno-heptopyranoses, glucoses, galactoses, and N-acetylglucosamine, partially substituted by one or two phosphate groups.<sup>28</sup> There are numerous articles about the chemical structures of core oligosaccharides and O-polysaccharides. For more details, the reader is referred to some excellent and exhaustive reviews.<sup>24,28,29</sup>

As endotoxins lack optically active groups, their detection in the underivatized state can be difficult. Therefore, Freitag and coworkers<sup>30</sup> have developed a capillary electrophoresis method and shown its potential for LPS analysis. Using standard phosphate buffers, concentrations down to 100 µg/mL can be detected within a few minutes. They showed, that the detection limit could be lowered by one order of magnitude by using a buffer containing sodium dodecylsulphate and borate. The low detection limit is due to the presence of the detergent, which homogenizes the LPS aggregates and to borate, which forms complexes with the molecules. In this way the optical activity is enhanced. The best results, in terms of detection limit and speed were obtained with an indirect UV-detection capillary electrophoresis method. A detection limit of ~3 µg/mL (35 pM) was obtained.<sup>30</sup> Recht and Kolter<sup>31</sup> investigated the sliding motility and biofilm formation of cells from *Mycobacterium smegmatis*. This ability to either attach to or slide over surfaces such as animal tissues can be important in the different stages of pathogenesis induced by the bacteria. They found that there is a nearly perfect correlation between the presence of a glycopeptidolipid GPL on the mycobacterial cell wall and the colony morphology, sliding motility, and biofilm formation.

Recently, Kislyuk and coworkers<sup>32</sup> used laser spectroscopy for the investigation of the structural components

(O-antigen, core oligosaccharide and lipid A) of lipopolysaccharides from *Ralstonia solanacearum* and rhizobial periplasmic glucans at extremely low concentrations ( $4\text{--}8 \times 10^{-2}\%$  water solutions of the glycopolymers). They showed, that the fluorescence and Raman spectra registered under UV laser excitation could help to distinguish different types of polysaccharides, which was impossible using optical absorption measurements due to the lower sensitivity. Kislyuk and coworkers concluded, that the spectra of the LPS structural components (vibrational structure) agree qualitatively with their conformations. An advantage of this method is that sample concentrations of physiological relevance can be used.

### 2.2.2. $\beta \leftrightarrow \alpha$ Acyl chain melting transition of endotoxins.

The determination of the  $T_c$  dependence on the chemical structures of the sugar moiety of LPS by various techniques showed for enterobacterial strains (natural salt-forms) the highest  $T_c$  values for free lipid A (around 45 °C), lowest for the deep rough mutant LPS (around 30 °C), and, with increasing length of the polysaccharide portion towards completion of the O-chain (wild-type LPS), increased again up to 37–40 °C.<sup>33–35</sup> In a systematic study, the dependence of the phase transition behaviour of LPS Re and lipid A preparations on changes in the number of Kdo and phosphate groups was investigated (Figs. 4 and 5). A clear correlation was found between the biological activity of the endotoxins—expressed as the amount necessary to induce a certain amount of cytokines—and the order parameter  $S$  (37 °C), which can be deduced from the peak position of the symmetric stretching vibration of the methylene groups as determined by IR-spectroscopy ( $S = 1$  for perfectly aligned and  $= 0$  for isotropically aligned molecules, Fig. 5).<sup>33</sup> This means that samples with the lowest  $S$  value (37 °C), corresponding to higher mobility or 'fluidity' of the acyl chains, have the highest biological activity.

For synthetic lipid A of *E. coli* and *S. minnesota* (compounds 506 and 516, respectively)  $T_c$ -values in close agreement with the natural compounds were found.<sup>37,38</sup>  $T_c$ -Values for various non-enterobacterial LPS and lipid A were usually significantly lower than those of *Enterobacteriaceae*.<sup>38</sup> This observation correlates with that the former often contain shorter acyl chains with a higher degree of unsaturation. In an infrared spectroscopic study, also the  $T_c$ -values and corresponding states of order of various lipid A analogues and partial structures were determined.<sup>37</sup> A characteristic dependence of  $T_c$  on the number of acyl chains was observed, with  $T_c$  lying significantly below 0 °C for the diacyl analogue '606', between 15 and 20 °C for the tetraacyl compound '406' corresponding to the lipid A precursor Ia or IVa, and at 43 °C for the hexaacyl compound '506'. The addition of divalent

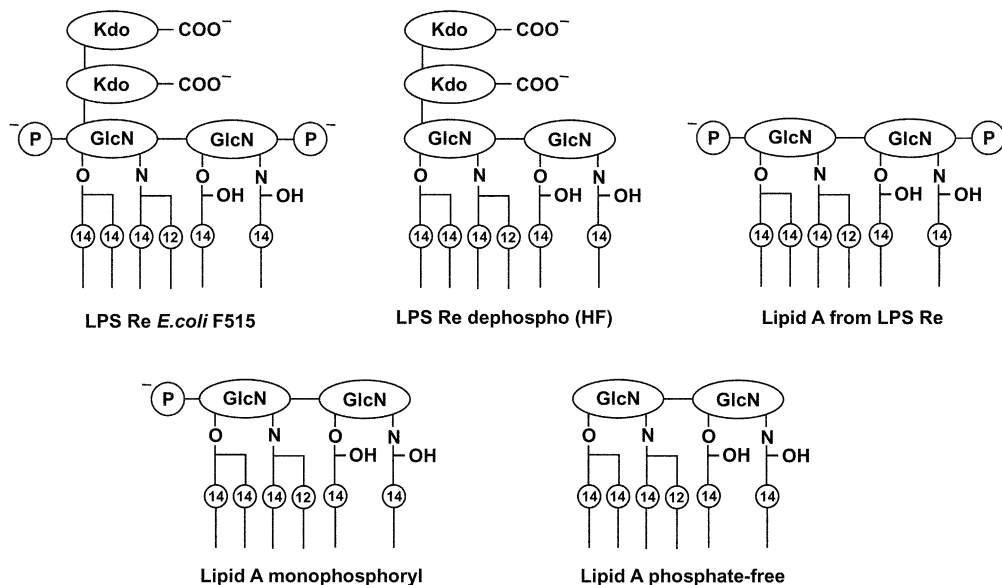


Fig. 4. Chemical structures of various LPS Re and lipid A part structures.

cations as well as a lowering of pH caused a significant rigidification of the acyl chains of free lipid A and LPS preparations and, partly, also led to an increase in  $T_c$ . At basic pH, a lowering of  $T_c$  was observed. Concomitant with a decrease of  $T_c$ , a fluidization of the LPS and lipid A acyl chains occurred.<sup>34</sup> Excess concentrations of  $Mg^{2+}$  led to an increase of  $T_c$  for LPS from *S. minnesota* and to LPS from *Erwinia carotovora* at [endotoxin]:[cation] = 1:1 M ( $Mg^{2+}$  or  $Ca^{2+}$ ).<sup>39,40</sup> The comparison of the influence of divalent cations on the phase behaviour of LPS Re showed a cation-specific increase of  $T_c$  in the sequence  $Mg^{2+} < Ni^{2+} < Co^{2+} <$

$Zn^{2+}$ , no matter, whether LPS dispersed in buffer or serum.<sup>40</sup>

**2.2.3. General ultrastructural studies.** Electron microscopy has become an essential tool in the identification and characterization of the morphological properties of endotoxins. In older papers on the aggregate structures of LPS<sup>41,42</sup> the impurity of the samples did not allow a reliable description, since contaminants such as proteins led to artefacts in the aggregate structure. Amano and coworkers<sup>43</sup> have used electron microscopy for the elucidation of structures of lipopolysaccharides from

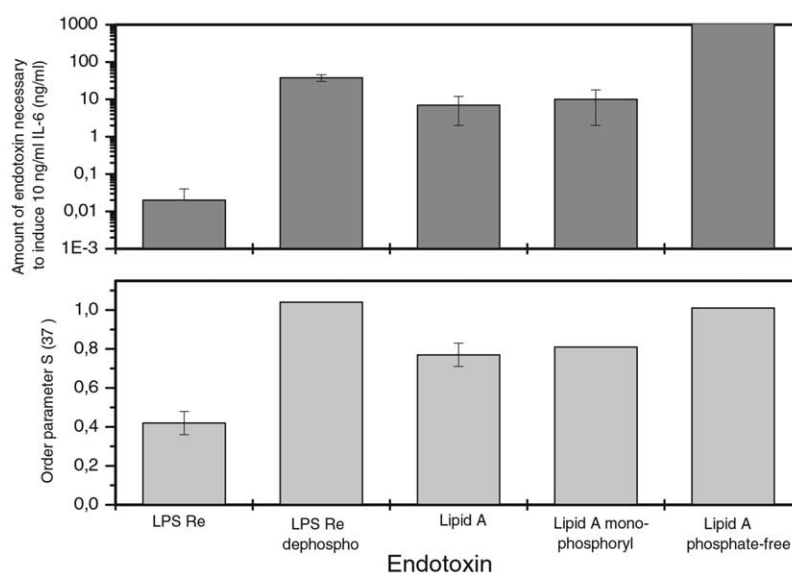


Fig. 5. Interleukin-6 inducing activity and the order parameter  $S$  (37 °C) of the acyl chains at 37 °C of various LPS Re and lipid A part structures. In the top figure, low values indicate high biological activity; in the bottom figure, low values indicate high mobility of the acyl chains.

phase I (LPSI) and II (LPSII) of *Coxiella burnetii*. The LPSI and LPSII ultrastructure of positively stained samples (with uranyl formate or uranyl acetate) was ribbon-like. When negatively stained with uranyl acetate, LPSI was ribbon-like but LPSII exhibited hexagonal lattice structures. However, LPSII stained negatively with sodium phosphotungstate and ammonium molybdate exhibited hexagonal lattice ultrastructures, which were not identical to those observed when negatively stained with uranyl acetate. The hexagonal lattice structures formed in vitro were due to the interactions of LPSII and the staining reagents rather than to protein-LPS interactions. The authors concluded, that the differences in the ultrastructures of LPSI and LPSII are undoubtedly based on variations in their chemical composition.<sup>43</sup>

The physico-chemical nature of the LPS aggregates used has a large impact on the physiological pathways in which endotoxin are involved. The morphology of the formed aggregates of commercial available LPS (from *E. coli* 0111:B4) in aqueous suspension was analysed by Risco and coworkers by negative staining and by platinum shadowing.<sup>44–46</sup> Different structures were observed. Staining with ammonium molybdate showed small aggregates and long ‘ribbons’. These filamentous ribbons branched freely and had an average diameter of 12 nm. The small aggregates that were distinguished in addition to the ribbon structures had a diameter between 10 and 50 nm. Shadowed endotoxin samples showed small globular aggregates (diameter 20–80 nm) and short filaments. However, the differences in the structures observed can be related to artefacts, as fusion of individual aggregates, are commonly associated with negative staining.<sup>43,47</sup> Sonication of this commercial LPS sample in normal serum did not result in more dispersed suspension. On the contrary, the aggregates became larger, and with a rough particulate internal texture. The later effect may be due to incorporation of serum proteins.<sup>44</sup> These large aggregates have a diameter of more than 200 nm and structures with several micrometer in length were detected.

Amphiphiles like glycolipids can self-aggregate (next paragraph), and the thermotropic and lyotropic liquid crystalline properties were extensively investigated. (Refs. 48, 49 and papers cited therein). It was found, that glycolipids exhibited hexagonal columnar mesophases. In the dry state, the aliphatic hydrocarbon chains were found to be located on the exterior of the columns, whereas in the wet, hydrated state the reverse was the case with the polar head groups on the exterior.<sup>48</sup> The formed superstructure depends mainly on the physico-chemical property of the investigated amphiphile. Naturally occurring galactocerebrosides derived from bovine brain adopt a wedge-like shape, which is determined by the chemical composition of the hydrophobic core as well as of the head group. These

physico-chemical properties are also observed for glycopolymers like lipooligo- and lipopolysaccharides.

It is known, that the physical aggregation state and thus presentation of LPS, including possible interactions with capsule, affect the ability of endotoxins to interact with and activate specific host targets. Giardina and coworkers<sup>50</sup> investigated the molecular determinants of host-meningococcal lipooligosaccharide (LOS, an endotoxin) interactions at pathophysiologically relevant endotoxin concentrations (i.e., < 10 ng/mL). Meningococcal lipid A consists of an *O*-phosphorylethanolamine-substituted  $\beta$ -(1'→6)-linked D-glucosamine backbone containing symmetrically arranged ester- and amide-linked 3-hydroxy fatty acids (3-OH FA).<sup>51</sup> The investigated glycopolymers were obtained from acetate auxotrophs NMBACE1 from encapsulated *Neisseria meningitidis* (serogroup B, strain NMB) and NMBACE2 from an isogenic bacterial mutant lacking the polysialic acid capsule. By GPC of metabolically labelled (<sup>14</sup>C) LOS, two major subpopulations of LOS were identified and separated, which exist in different aggregation forms. The broad resolving range of the used gel column Sephacryl S500 was particularly important as aggregates can be present that vary in apparent molecular mass from 1–20 × 10<sup>6</sup> Da and bioactive complexes containing LOS are ~ 10<sup>5</sup> Da. The molecular mass of the aggregates from both strains (NMBACE1 and NMBACE2) was estimated being larger than > 20 × 10<sup>6</sup> and ~ 1 × 10<sup>6</sup> Da, respectively. Lipooligosaccharides found in both fractions had the same fatty acid composition and SDS-polyacrylamide gel electrophoresis (PAGE) profile.

Using biological assays, these data allow an assessment of the effect of aggregation state on the biochemical reactivity and biological activity of LOS.<sup>50</sup> This is in accordance to data reported by Kitchens and Munford.<sup>52</sup> They reported that bacterial LPS (*E. coli*) is internalized by a constitutive cellular mechanism (CD14-dependent) with kinetics depending importantly upon the physical state in which the LPS is presented to the cell.

Also, the clearance of LPS depends on the aggregation form. It was found that aggregates of LPS were internalized in association with mCD14, suggesting that LPS clearance occurs via a pathway distinct from that which leads to signalling via LPS.<sup>53</sup>

Giwerzman and coworkers<sup>54</sup> were able to show, by PAGE, differences in the physico-chemical properties of lipopolysaccharide from *Pseudomonas aeruginosa* extracted from biofilm and plankton. The latter were grown as strain of monoagglutinable (1118) and polyagglutinable (258 and 15703), which were isolated from cystic fibrosis patients with chronic pulmonary infections. Analysis by PAGE followed by immune-detection of LPS fractions showed an S-form appearance of strain 1118 and 258 with three distinct clusters of high

molecular weight bands, whereas 15703 appeared semi-rough. LPS of semi-rough cells grown in plankton and as biofilm showed a similar PAGE pattern; however, the core/lipid A R-LPS fraction was more prominent in biofilm-LPS than in plankton-LPS extracted from the S-form bacteria (1118 and 258).

It is known, that in lipid A, the number and position of fatty acids influence the permeability barrier of the bacteria as well as the toxicity of the LPS.<sup>55–57</sup> The chemical composition and structure of *P. aeruginosa* lipid A demonstrates hexacyl as well as predominantly pentaacyl components, which is fewer than the six to seven fatty acids found in *Enterobacteriaceae*.<sup>57,58</sup> Moreover, the number of fatty acids seems to differ in lipid A of the high and low molecular weight LPS fractions with the highest number of fatty acids being in the lower-molecular weight LPS fractions.<sup>56,59</sup> Thus, the biofilm of the apparent S-form *P. aeruginosa* strains contains increased amounts of low molecular weight core/lipid A fractions and higher amounts of fatty acids. The demonstrated increase in R-form LPS fractions in *P. aeruginosa* biofilm may directly contribute to an altered permeability barrier toward lipophilic solutions, a change in endotoxic properties, and influence the bacterial binding to plastic surfaces.

Giwerzman and coworkers<sup>54</sup> concluded that the apparent change in LPS subunit components of the bacteria when grown as biofilm may reflect changes in the outer membrane structure that contributes to the altered physico-chemical properties of biofilm bacteria.

**2.2.4. CMC and aggregate structure of endotoxins.** No exact value for CMC of lipid A or LPS has been published so far, which seems to be due to extreme experimental difficulties in the low concentration range, e.g., working close to the detection limits, loss of material from absorption to surfaces, etc. A rough estimation, however, can be given from the limited number of available data for other lipids. In a paper of Hofer and coworkers<sup>60</sup> a value of  $<10^{-7}$  M for the lipid A precursor lipid IVa (tetraacyl lipid A corresponding to synthetic compounds ‘406’) was found from which a value significantly lower than  $10^{-8}$  M for lipid A can be estimated. This is in accordance with preliminary and unpublished data from our laboratory, and is also backed by data on the ‘solubility’ of LPS Re determined experimentally applying equilibrium dialysis by Takayama and coworkers.<sup>61</sup> The authors found saturation values of the solubility of  $3.3 \times 10^{-8}$  M at 22 °C and  $2.8 \times 10^{-8}$  M at 37 °C. Previously, one paper has been published in which the authors claim to have determined the ‘critical aggregation concentration’ (CAC, taken as synonym for CMC) of lipid A and LPS.<sup>62</sup> However, their results of CACs, lying in the range 4–10  $\mu$ M for different endotoxins, reflect the sensitivity limit of the applied measuring techniques

with fluorescence using *N*-phenyl naphtylamine and 90° light scattering rather than the CAC or CMC. We have found that for various phospholipids (among others dimyristoylphosphatidylcholine, dipalmitoylphosphatidylcholine, and distearoylphosphatidylcholine) as well as endotoxins (lipid A and various rough and smooth form LPS from *S. minnesota* with differently long sugar chains) analysed by fluorescence spectroscopy with a variety of dyes and 90°-light scattering, the signals all disappear in the micromolar range, although the values of the CMC should diverge by orders of magnitude for the different lipids (unpublished results).

Santos and coworkers<sup>63</sup> used CMC in a different sense. They defined  $CMC_a$  as a transition value from a premicellar to a micellar structure (‘micellar’ as synonym for aggregate), by using dynamic and static light scattering for the direct characterization of these aggregates. They obtained  $CMC_a$  for LPS from *E. coli* (serotype 026:B6) of 14  $\mu$ g/mL, which is not far away from the artificial data published by Aurell and Wistrom.<sup>62</sup> Using static light scattering, different physical parameters of the aggregates could be calculated as the molecular weight (MW), the second virial coefficient ( $A_2$ ) and the gyration radius ( $R_g$ ). It was found, that the MW value above  $CMC_a$  is approximately three times larger compared to the MW value below  $CMC_a$  (Table 1). This result suggests the formation of ‘trimers’ of the units present below  $CMC_a$ . Santos and coworkers concluded from their results the existence of premicellar LPS structures below  $CMC_a$  (of course, these premicellar structures are still aggregates). The negative  $A_2$  data signify a poor interaction between LPS and the aqueous solvent, which point to a tendency towards self-aggregation. The increase of  $A_2$  for concentrations larger than  $CMC_a$  indicates better interactions with the bulk solvent. This can be realized by a better and more

Table 1

Physical parameters obtained by light scattering of LPS (*E. coli*, serotype 026:B6) above and below the CMC (transition into a less aggregated form,  $CMC_a = 14 \mu$ g/mL, see text) in PBS (pH 7.4) at 37 °C

Physical parameter	LPS concentration < $CMC_a$	LPS concentration > $CMC_a$
MW (g mol <sup>-1</sup> )	$5.5 \pm 0.6 \times 10^6$	$16.0 \pm 1.6 \times 10^6$
$A_2$ (cm <sup>3</sup> mol g <sup>-1</sup> )	$-42.8 \pm 2.1$	$-0.68 \pm 0.03$
$R_g$ (nm)	$56 \pm 7$	$105 \pm 13$
$R_h$ (nm)	$60 \pm 3$	$95 \pm 5$
$\rho = R_g/R_h$	$0.86 \pm 0.11$	$1.10 \pm 0.14$

With: MW = molecular weight,  $A_2$  = second virial coefficient,  $R_g$  = gyration radius,  $R_h$  = hydrodynamic radius. The given error boundaries are the standard deviations (adapted from Santos and coworkers 2003)<sup>63</sup>



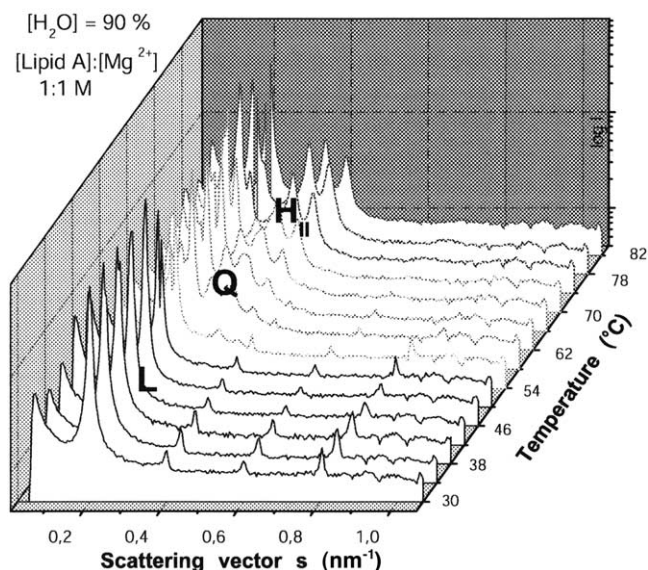


Fig. 6. Synchrotron radiation X-ray diffraction patterns of lipid A from *S. mimesota* deep rough mutant LPS Re in dependence on temperature at 85% water content and [lipid A]:[Mg<sup>2+</sup>] = 1:1 molar. The patterns indicate a triphasic behaviour with a multilamellar (L) structure at lower, a cubic (Q) structure at medium, and an inverted hexagonal (H<sub>II</sub>) structure at the highest temperatures.

effective shielding of hydrophobic LPS parts from the polar aqueous phase and by increased intermolecular

interactions upon micelle formation.<sup>63</sup> The dimension of the formed aggregates are similar for concentrations below and above CMC<sub>a</sub> (see Table 1), and in both cases nearly spherical structures were formed.

Generally, the aggregate structure of amphiphilic molecules above CMC can be assessed by a simple geometric model, which relates the resulting structure to the ratio of the effective cross-sectional areas,  $a_o$ , of the hydrophilic polar and,  $a_h$ , the hydrophobic apolar regions, respectively. A dimensionless shape parameter  $S = v/(a_o A l_c) = a_h/a_o$  ( $v$  volume per molecule of the hydrophobic moiety,  $l_c$  length of the fully extended hydrophobic portion) was introduced by Israelachvili.<sup>26</sup> From this value, which may be estimated for example from energy minimization calculations, a predicted structure of the supramolecular aggregates can be deduced.

Amphiphiles with shape parameters in the range  $\frac{1}{2} < S < 1$  assume lamellar (L) structures, and those with a prominent axis of the head-group and  $S > 1$  adopt inverted hexagonal (H<sub>II</sub>) structures. In the latter case, the water component is assumed to form idealized circular rods lined with the hydrated lipid backbones and with the remaining volume filled by the fluid hydrocarbon chains. Another category are the cubic (Q) structures, which have three-dimensional geometry and cannot be described by a unique structure<sup>64</sup> other

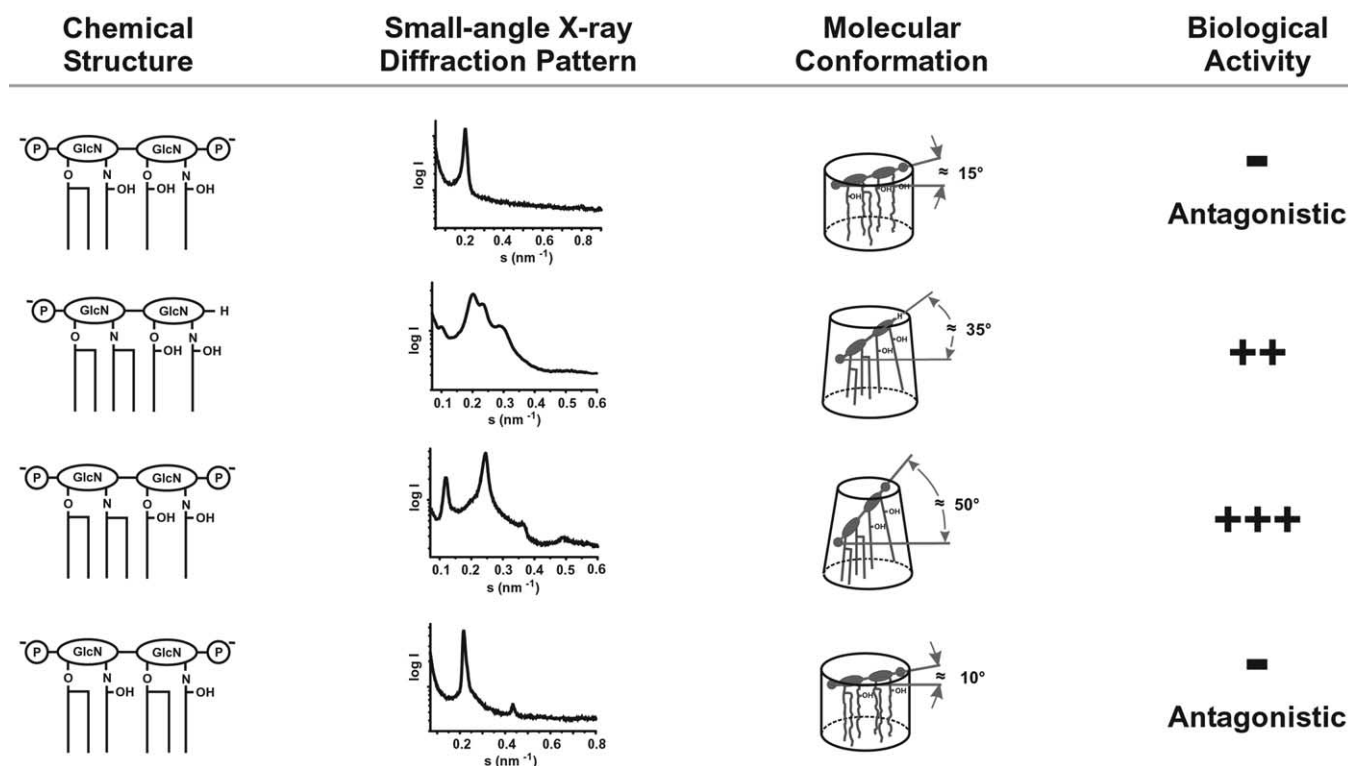


Fig. 7. Chemical structures, X-ray diffraction patterns, molecular conformation, and biological activity of various lipid A and part structures.

Table 2

Aggregate structure, order parameter  $S$  (37 °C), phase transition temperature  $T_c$ , and the relative biological activity for lipid A structures from different origin (according to Ref. 72 and unpublished results)

Bacterial species	Lipid A structural features as compared to <i>E.coli</i> -lipid A	Three-dimensional structure	$S$ (37 °C)	$T_c$ (°C)	Relative endotoxic activity
<i>C. jejuni</i>	acyl chains longer (C-16)	Main: Q minor: L	0.84	52	medium
<i>C. burnetii</i>	tetraacyl, C-16 acyl chains and longer	Q	0.39	20	medium
<i>C. violaceum</i>	symmetric 3,3 linkage of acyl chains	L	0.30	25	absent, antagonistic
<i>E. coli</i>		Q	$0.73 \pm 0.04^b$	43	high
<i>E. coli</i> , mutant	pentaacyl: 3- <i>O</i> acyl group lacking at 3' position	L	0.40	32	absent, antagonistic
<i>P. aeruginosa</i>	mainly pentaacyl component	predominantly L	0.28	<sup>a</sup>	low
<i>P. fluorescense</i>	mainly pentaacyl component	L	n.d.	n.d.	low
<i>P. mirabilis</i> Re45	additional arabinose in headgroup	Q	0.80	49	high
<i>Rb.capsulatus</i>	only five acyl chains with shorter chain lengths including one unsaturated chain	L	0.27	< –	absent, antagonistic
<i>Rs. Fulvum</i>	GalA instead of 1-P, heptose instead of 4'-P, acyl chains slightly longer	L	0.70	40	low
<i>Rc. gelatinosus</i>	acyl chain lengths distinctly shorter (C-10, C-12)	H <sub>II</sub>	0.15	< –	high
<i>Rm. vannielii</i>	probably pentaacyl, no charges	L	n.d.	n.d.	absent
<i>Rp. Viridis</i>	not in all details known, contains long (C-28:0) acyl chains	L	0.35	32	absent
<i>R. sphaeroides</i> (synthetic)	pentaacyl, C14:1 in 2' linkage, shorter chains	L	0.18	< –	absent, antagonistic
<i>S. minnesota</i> mono-phosphoryl	4'-phosphate group absent	Q/L	0.81	44	medium
<i>S. minnesota</i>	heptaacyl component in substoichiometric amounts	Q	$0.78 \pm 0.04^b$	46	high
<i>S. minnesota</i> (Ca-salt)		L	0.81	46	absent
<i>S. paucimobilis</i>	glycosphingolipid instead of lipid A	L			absent
	GSL-1: monosaccharide	L/Q	0.58 <sup>a</sup>	0.33 <sup>a</sup>	low
	GSL-4: tetrasaccharide	L	0.23	25	absent, antagonistic
Precursor '406'	tetraacyl	L	0.23	25	absent, antagonistic
505	1-monophosphoryl	Q	0.84	48	relatively high
CM-506	carboxymethyl instead of 1-phosphate	Q	0.90	50	high
Lipid X	reducing part of lipid A	L	n.d.	n.d.	absent, medium antagonistic

L = lamellar, Q = cubic and H<sub>II</sub> = inverted hexagonal structures. n.d. not determined.

<sup>a</sup> No sharp transition.

<sup>b</sup> Standard deviation from five different batches.

than the L and H<sub>II</sub> phases, which have one- or two-dimensional geometry, respectively.

In previous investigations, complete phase diagrams were established for lipid A, LPS Re, and other rough mutant LPS from *S. minnesota* and *E. coli* over a wide range of water content (20–95%), Mg<sup>2+</sup> concentrations (molar ratio [lipid]:[Mg<sup>2+</sup>] from 1:0 to 1:1), and dependence on temperature.<sup>65–67</sup> The phase diagrams include the determination of the aggregate structures with synchrotron radiation X-ray scattering (SAXS) and that of the phase behaviour with Fourier-transform

infrared spectroscopy (FTIR). As an example of the structural variability of the endotoxins (Fig. 6), the temperature dependence of the X-ray diffraction patterns is shown for a lipid A from *Salmonella minnesota* exhibiting a triphasic behaviour with a lamellar (L) structure at lower, a cubic (Q) structure at medium, and an inverted hexagonal (H<sub>II</sub>) structure at higher temperatures. Summarizing the results for the phase diagrams, it can be stated that free lipid A adopts lamellar structures at water contents below ~60% and undergoes a transition into non-lamellar cubic structures at higher

water concentrations already below  $T_c$ . In other words, a lyotropic structural transition takes place around 60% water content.<sup>65</sup> Similar observations were made for deep rough mutant LPS Re,<sup>66</sup> but for other rough mutant LPS the tendency to assume only lamellar structures at  $T < T_c$  increases.<sup>67</sup> In the presence of divalent cations (e.g.,  $Mg^{2+}$ ) in a lipid to cation molar ratio of 1, non-lamellar structures are suppressed below  $T_c$ . At the same time,  $T_c$  is shifted to higher values (see previous section). Once the acyl chain melting process begins, free lipid A assumes non-lamellar cubic structures over the whole range of water contents. With the completion of chain melting, the cubic structures change into inverted hexagonal  $H_{II}$  structures. For deep rough mutant LPS, the situation is similar in that with the chain melting a transition into non-lamellar cubic structures takes place, but the transition into  $H_{II}$  occurs at considerably higher temperatures ( $> 70^\circ C$ ).<sup>66</sup> The tendency for other rough mutant LPS to adopt non-lamellar structures at and above  $T_c$  decreases with increasing completeness of the core region. The presence of divalent cations at concentrations as described above suppresses the formation of non-lamellar cubic structures. Measurements of the aggregate structure were extended to other lipid A samples, e.g., enterobacterial LPS and lipid A in different salt forms, monophosphoryl lipid A, and lipid A from non-enterobacterial sources like those of *Rhodobacter capsulatus*, *Rhodopseudomonas viridis*, *Rhodocyclus* (new classification: *Rubrivivax*) *gelatinosus*, *Rhodospirillum fulvum*, *Campylobacter jejuni* and *Chromobacterium violaceum*<sup>25</sup> under near physiological conditions with the purpose of directly correlating the results to data from biological test systems. It was found that different non-enterobacterial lipid A samples showed a variety of aggregate structures ranging from  $H_{II}$  (lipid A from *Rc. gelatinosus*) over mixed cubic/lamellar (monophosphoryl lipid A from *S. minnesota* and lipid A from *C. jejuni*) to pure lamellar structures (lipid A from *C. violaceum*, *Rb. capsulatus*, *Rp. viridis*, and *Rs. fulvum*). Interestingly, the triacyl lipid A part structure OM-174 with a normal disaccharide backbone exhibited also a non-lamellar, but not inverted ( $H_I$ ) structure, connected with lower, but not vanishing activity in the cytokine assay.<sup>68</sup> Also synthetic triacyl monophosphoryl synthetic lipid A partial structures were investigated and showed a specific dependence of the aggregate structure and the intramolecular conformation (see next paragraph) from the binding sites to the sugar backbone.<sup>69</sup>

By applying FTIR spectroscopy using an attenuated total reflectance unit with polarized IR light, the orientation of molecular groups within lipid A could be determined.<sup>70</sup> Enterobacterial lipid A shows a strong inclination of the diglucosamine backbone (normal to the sugar plane) with respect to the direction of the hydrocarbon chains of more than  $45^\circ$ , whereas lower

acylated lipid A (penta- and tetra-) as well as some non-enterobacterial lipid A exhibited a much lower angle ( $< 20^\circ$ ). Monophosphoryl lipid A (4'-phosphoryl lipid A corresponding to synthetic 504) has an intermediate inclination ( $36\text{--}38^\circ$ ). Accordingly, the backbone of lipid A with a conical shape is strongly inclined, that with an only slight conical shape has a medium inclination, and that with a cylindrical shape has—if at all—only a slight inclination. It should be emphasized that the two parameters, molecular shape and inclination are interdependent, and apparently express the packing constraints of the hydrocarbon chains with respect to the available cross sectional areas, and determine, most importantly, also the ability of lipid A to act agonistically or antagonistically.

**2.2.5. Correlations to bioactivity.** As stressed already above (see Figs. 4 and 5), correlations between the phase transition temperature or the order parameter  $S$  ( $37^\circ C$ ), respectively, and various biological effects have been found.<sup>41,71</sup> It must be emphasized, however, that a high acyl chain fluidity is not a priori a determinant of bioactivity. LPS such as that from *Rb. capsulatus* are known with a lipid A having highly fluid hydrocarbon chains but no biological activity.<sup>36</sup>

From the foregoing, it can be stated that a basic quantity, which is an important determinant of endotoxicity, is the aggregate structure of lipid A. This quantity was described to be a measure of the molecular conformation ('conformational concept').<sup>25,71–73</sup> Together with the data from the determination of the intramolecular conformation, a schematic of the intrinsic conformation of biologically active and inactive lipid A can be given: Hexaacyl lipid A with an asymmetric acyl chain distribution, a high inclination angle, and a conical shape have highest activity, followed by monophosphoryl lipid A, while all other samples with low inclination and cylindrical conformation are inactive, but act antagonistically (Fig. 7). Similar data were obtained for the monosaccharide monophosphoryl triacyl lipid A structures mentioned above, those compounds with a acyloxyacyl chain in position 3 had a non-lamellar aggregate structure and exhibited bioactivity (but significantly lower than entire lipid A), whereas those compounds with the acyloxyacyl chain linked to position 2 were inactive.<sup>69</sup> Data on the aggregate structure as well as the relative biological activities are summarized in Table 2, in which  $S$  ( $37^\circ C$ ) and the  $T_c$  values are given (Ref. 72 and unpublished results). As can be deduced from the table, there seems to exist a clear correlation between the preference of lipid A to adopt particular aggregate structures and their biological action: All lipid A with a preference for cubic inverted structures are highly active, those with a lamellar structure are inactive. The latter, however may

be antagonistically active, i.e., may be able to block the action of agonistically compounds.

## Acknowledgements

This work was financially supported by the Deutsche Forschungsgemeinschaft (SFB 367, project B8) and the European Union (project ANEPID).

## References

- Curatolo, W. *Biochim. Biophys. Acta* **1987**, *906*, 137–160.
- Lingwood, C. A. *Curr. Opin. Struct. Biol.* **1992**, *2*, 693–700.
- Hooper, N. M. *Curr. Biol.* **1998**, *8*, R114–R116.
- Rietschel, E. T.; Brade, H.; Holst, O.; Brade, L.; Müller-Loennies, S.; Mamat, U.; Zähringer, U.; Beckmann, F.; Seydel, U.; Brandenburg, K.; Ulmer, A. J.; Mattern, T.; Heine, H.; Schletter, J.; Hauschildt, S.; Loppnow, H.; Schönbeck, U.; Flad, H.-D.; Schade, U. F.; DiPadova, F.; Kusumoto, S.; Schumann, R. R. *Curr. Top. Microbiol. Immunol.* **1996**, *216*, 39–81.
- Crescenzi, V. *Biotechnol. Prog.* **1995**, *11*, 251–259.
- Brandenburg, K.; Seydel, U. In *Handbook of Vibrational Spectroscopy*; Chalmers, J. M.; Griffiths, P. R., Eds. Vibrational spectroscopy of carbohydrates and glycoconjugates; Vol. 5; Wiley and Sons: Chichester, 2002; pp 3481–3507.
- Ashwell, G. *Methods Enzymol.* **1957**, *3*, 73–105.
- Chen, P. S.; Toribara, T. Y.; Warner, H. *Anal. Chem.* **1956**, *28*, 1756–1758.
- Anderson, P.; Pichichero, M. E.; Insel, R. A. *J. Clin. Invest.* **1985**, *76*, 52–59.
- Kabat, E. A.; Mayer, M. M. *Experimental Immunochimistry*; 2nd ed.; Thomas C. C: Springfield, IL, 1961.
- Svennerholm, L. *Biochem. Biophys. Acta* **1957**, *24*, 604–611.
- Hestrin, S. *J. Biol. Chem.* **1949**, *180*, 249–261.
- Nash, T. *J. Biochem.* **1953**, *55*, 416–421.
- Lifely, M. R.; Nowicka, U. T.; Moreno, C. *Carbohydr. Res.* **1986**, *156*, 123–135.
- Chen, F.-T. A.; Dobashi, T. S.; Evangelista, R. A. *Glycobiology* **1998**, *8*, 1045–1052.
- Inoue, S.; Lin, S.-L.; Lee, Y. C.; Inoue, Y. *Glycobiology* **2001**, *11*, 759–767.
- Anumula, K. R.; Dhume, S. T. *Glycobiology* **1998**, *8*, 685–694.
- Sato, N.; Nakazawa, F.; Ito, T.; Hoshino, T.; Hoshino, E. *Carbohydr. Res.* **2003**, *338*, 923–930.
- Varbanets, L. D.; Shashkov, A. S.; Kocharova, N. A. *Carbohydr. Res.* **1990**, *204*, 157–160.
- Ravenscroft, N.; Averani, G.; Bartoloni, A.; Berti, S.; Bigio, M.; Carinci, V.; Costantino, P.; D'Ascenzi, S.; Giannozzi, A.; Norelli, F.; Pennatini, C.; Proietti, D.; Ceccarini, C.; Cescutti, P. *Vaccine* **2002**, *17*, 2802–2816.
- Costantino, P.; Norelli, F.; Giannozzi, A.; D'Ascenzi, S.; Bartoloni, A.; Kaur, S.; Tang, D.; Seid, R.; Viti, S.; Paffetti, R.; Bigio, M.; Pennatini, C.; Averani, G.; Guarnieri, V.; Gallo, E.; Ravenscroft, N.; Lazzeroni, C.; Rappuoli, R.; Ceccarini, C. *Vaccine* **2002**, *17*, 1251–1263.
- Bussat, B.; Schulz, D.; Arminjon, F.; Valentin, C.; Armand, J. *Biologicals* **1990**, *18*, 117–121.
- Baumgart, T.; Offenhäusser, A. *Langmuir* **2003**, *19*, 1730–1737.
- Wilkinson, S. G. *Prog. Lipid Res.* **1996**, *35*, 283–343.
- Schromm, A. B.; Brandenburg, K.; Loppnow, H.; Moran, A. P.; Koch, M. H. J.; Rietschel, E. T.; Seydel, U. *Eur. J. Biochem.* **2000**, *267*, 2008–2013.
- Intermolecular and Surface Forces*; Israelachvili, J. N., Ed.; 2nd ed.; Academic Press: London, 1991; p 366.
- Holst, O.; Ulmer, A. J.; Brade, H.; Flad, H. D.; Rietschel, E. T. *FEMS Immunol. Med. Microbiol.* **1996**, *16*, 83–104.
- Holst, O. In *Endotoxin in Health and Disease*; Brade, H.; Opal, S. M.; Vogel, S. N.; Morrison, D. C., Eds. Chemical structure of the core region of lipopolysaccharides; Marcel Dekker, Inc: New York, 1999; pp 115–154.
- Jansson, P.-E. In *Endotoxin in Health and Disease*; Brade, H.; Opal, S. M.; Vogel, S.; Morrison, D. C., Eds. The chemistry of O-polysaccharide chains in bacterial lipopolysaccharides; Marcel Dekker: New York, 1999; pp 155–178.
- Freitag, R.; Fix, M.; Brüggemann, O. *Electrophoresis* **1997**, *18*, 1899–1905.
- Recht, J.; Kolter, R. *J. Bacteriol.* **2001**, *183*, 5718–5724.
- Kislyuk, V. V.; Varbanets, L. D.; Kosenko, L. V.; Vasiliev, V. N.; Vinarskaya, N. V.; Pahuta, I. M.; Lozovski, V. Z. *Synth. Met.* **2002**, *127*, 23–28.
- Brandenburg, K.; Seydel, U. *Biochim. Biophys. Acta* **1984**, *775*, 225–238.
- Brandenburg, K.; Seydel, U. *Eur. J. Biochem.* **1990**, *191*, 229–236.
- Naumann, D.; Schultz, C.; Sabisch, A.; Kastowsky, M.; Labischinski, H. *J. Mol. Struct.* **1989**, *214*, 213–246.
- Brandenburg, K.; Mayer, H.; Koch, M. H. J.; Weckesser, J.; Rietschel, E. T.; Seydel, U. *Eur. J. Biochem.* **1993**, *218*, 555–563.
- Naumann, D.; Schultz, C.; Born, J.; Labischinski, H.; Brandenburg, K.; von Busse, G.; Brade, H.; Seydel, U. *Eur. J. Biochem.* **1987**, *164*, 159–169.
- Brandenburg, K.; Kusumoto, S.; Seydel, U. *Biochim. Biophys. Acta* **1997**, *1329*, 193–201.
- Fukuoka, S.; Brandenburg, K.; Müller, M.; Lindner, B.; Koch, M. H. J.; Seydel, U. *Biochim. Biophys. Acta* **2001**, *1510*, 185–197.
- Wellinghausen, N.; Schromm, A. B.; Seydel, U.; Brandenburg, K.; Luhm, J.; Kirchner, H.; Rink, L. *J. Immunol.* **1996**, *157*, 3139–3145.
- Seydel, U.; Brandenburg, K. In *Bacterial Endotoxin Lipopolysaccharides*; Morrison, D. C.; Ryan, J., Eds. Supramolecular structure of lipopolysaccharides and lipid A; CRC Press: Boca Raton, 1992; pp 225–250.
- Seydel, U.; Labischinski, H.; Kastowsky, M.; Brandenburg, K. *Immunobiology* **1993**, *187*, 191–211.
- Amano, K.; Fukushi, K.; Williams, J. C. *J. Gen. Microbiol.* **1985**, *131*, 3127–3130.
- Risco, C.; Pinto Da Silva, P. *J. Histochem. Cytochem.* **1993**, *41*, 601–608.



45. Andersson-Forsman, C.; Pinto Da Silva, P. *J. Cell. Sci.* **1988**, *36*, 1413–1418.
46. Risco, C.; Dominguez, J. E.; Bosch, M. A.; Carrascosam, J. L. *Mol. Cell Biochem.* **1993**, *121*, 67–74.
47. Brogden, K. A.; Phillipis, M. *Electron Microscop. Rev.* **1988**, *1*, 261–278.
48. Dumoulin, F.; Lafont, D.; Boullanger, P.; Mackenzie, G.; Mehl, G. H.; Goodby, J. W. *J. Am. Chem. Soc.* **2002**, *124*, 13737–13748.
49. Lecollinet, G.; Gulik, A.; Mackenzie, G.; Goddby, J. W.; Benvegna, T.; Plusquellec, D. *Chem. Eur. J.* **2002**, *8*, 585–593.
50. Giardina, P. C.; Gioannini, T.; Buscher, B. A.; Zaleski, A.; Zhengi, D.-S.; Stolli, L.; Teghanemti, A.; Apicella, M. A.; Weiss, J. *J. Biol. Chem.* **2001**, *276*, 5883–5891.
51. Kulshin, V. A.; Zahringer, U.; Lindner, B.; Frasc, C. E.; Tsai, C. M.; Dmitriev, B. A.; Rietschel, E. T. *J. Bacteriol.* **1992**, *174*, 1793–1800.
52. Kitchens, R. L.; Munford, R. S. *J. Immunol.* **1998**, *160*, 1920–1928.
53. Vasselon, T.; Hailman, E.; Thieringer, R.; Detmers, P. A. *J. Exp. Med.* **1999**, *190*, 506–521.
54. Giwerzman, B.; Fomsgaard, A.; Mansa, B.; Hoiby, N. *Microbiol. Immunol.* **1992**, *89*, 225–230.
55. Vaara, M.; Nikaïdo, H. In *Handbook of Endotoxins*; Rietschel, E. T., Ed. Molecular organization of bacterial outer membranes; Vol. 1; Elsevier: New York, 1984; pp 1–45.
56. Galanos, C.; Jiao, B.; Kumoro, T.; Freudenberg, M. A.; Liideritz, O. *J. Chromatogr.* **1988**, *440*, 397–404.
57. Rietschel, E. T.; Brade, L.; Hoist, O.; Kulshin, V. A.; Linder, B.; Moran, A. P.; Schade, U. F.; Zähringer, U.; Brade, H. In *Cellular and Molecular Aspects of Endotoxin Reactions*; Nowonotny, A.; Spitzer, J. J.; Ziegler, E. J., Eds. Molecular structure of bacterial endotoxin in relation to bioactivity; Excerpta Medica: New York, 1990; pp 15–32.
58. Fomsgaard, A.; Conrad, R. S.; Galanos, C.; Shand, G. H.; Hoiby, N. *J. Clin. Microbiol.* **1988**, *26*, 821–826.
59. Fomsgaard, A.; Freudenberg, M. A.; Galanos, C. *J. Clin. Microbiol.* **1990**, *28*, 2627–2631.
60. Hofer, M.; Hampton, R. Y.; Raetz, C. R. H.; Yu, H. *Chem. Phys. Lipids* **1991**, *59*, 167–181.
61. Takayama, K.; Mitchell, D. H.; Din, Z. Z.; Mukerjee, P.; Li, C.; Coleman, D. L. *J. Biol. Chem.* **1994**, *269*, 2241–2244.
62. Aurell, C. A.; Wistrom, A. O. *Biochem. Biophys. Acta Res. Commun.* **1998**, *253*, 119–123.
63. Santos, N. C.; Silva, A. C.; Castanho, M. A. R. B.; Martins-Silva, J.; Salanha, C. *Chem. Bio. Chem.* **2003**, *4*, 96–100.
64. Luzzati, V. *Curr. Opin. Struct. Biol.* **1997**, *7*, 661–668.
65. Brandenburg, K.; Koch, M. H. J.; Seydel, U. *J. Struct. Biol.* **1990**, *105*, 11–21.
66. Brandenburg, K.; Koch, M. H. J.; Seydel, U. *J. Struct. Biol.* **1992**, *108*, 93–106.
67. Seydel, U.; Koch, M. H. J.; Brandenburg, K. *J. Struct. Biol.* **1993**, *110*, 232–243.
68. Brandenburg, K.; Lindner, B.; Schromm, A. B.; Koch, M. H. J.; Bauer, J.; Merkli, A.; Zbaeren, C.; Davies, J. G.; Seydel, U. *Eur. J. Biochem.* **2000**, *267*, 3370–3377.
69. Brandenburg, K.; Matsuura, M.; Heine, H.; Müller, M.; Kiso, M.; Ishida, H.; Koch, M. H. J.; Seydel, U. *Biophys. J.* **2002**, *83*, 322–333.
70. Seydel, U.; Oikawa, M.; Fukase, K.; Kusumoto, S.; Brandenburg, K. *Eur. J. Biochem.* **2000**, *267*, 3032–3039.
71. Seydel, U.; Wiese, A.; Schromm, A. B.; Brandenburg, K. In *Endotoxin in Health and Disease*; Morrison, D.; Brade, H.; Opal, S.; Vogel, S., Eds. A biophysical view on the function and activity of endotoxins; Marcel Dekker: New York, 1999; pp 195–220.
72. Brandenburg, K.; Seydel, U.; Schromm, A. B.; Loppnow, H.; Koch, M. H. J.; Rietschel, E. T. *J. Endotoxin Res.* **1996**, *3*, 173–178.
73. Schromm, A. B.; Brandenburg, K.; Loppnow, H.; Zähringer, U.; Rietschel, E. T.; Carroll, S. F.; Koch, M. H. J.; Kusumoto, S.; Seydel, U. *J. Immunol.* **1998**, *161*, 5464–5471.